Supplementary Information

Degradation and Regeneration of Hybrid Perovskites

*Charu Seth and Deepa Khushalani**

Materials Chemistry Research Group, Department of Chemical Sciences, Tata Institute of Fundamental Research, Homi Bhabha Rd, Colaba, Mumbai, India 400005

Table S1. A summary of the studies on instability of HOIP

Title of the paper[ref]	Degradation conditions	Technique used	Type of sample/cell	Major conclusions
Stability of solution-processed $MAPbI_3$ and $FAPbI_3$ layers[1]	Thermal degradation (ambient and inert)	Time evolution of XRD peaks	$MAPbI_3/TiO_2$/corning glass	Degradation catalyzed by water but happens in the absence of water too
The interaction between perovskite and selective contacts in perovskite solar cells: an IR study[2]	Moisture influence ($MAPbI_3$ deposited on TiO_2, Al_2O_3, ZnO)	IR, XRD	Hole-transporter/$MAPbI_3$/substrate/Si	Hole transporter protects perovskite; substrate affects morphology and stability
Light-activated photocurrent degradation and self-healing in perovskite solar cells[3]	Light	Meta stable states using CV, photocurrent transient measurement, IR, impedance	ITO/PEDOT:PSS/$MAPbI_3$/PCBM/Al	Light activated meta-stable states leads to charged regions in bulk; these states dissipate away in dark Proposed reason: polaron formation (theoretical)
Is Excess PbI_2 Beneficial for Perovskite Solar Cell Performance?[4]	PbI_2, O_2 and moisture, illumination	XRD, PCE	MoO_3-Al /spiro-OMeTAD /$CH_3NH_3PbI_3/TiO_2$/FTO	PbI_2 affects morphology; enhances photodegradation
Parameters responsible for the degradation of $CH_3NH_3PbI_3$-based solar cells on polymer substrates[5]	Light, temperature, humidity, hole transporter, O_2	PCE, XRD	Au/hole-transporter /$CH_3NH_3PbI_3/TiO_2$/In doped ZnO	Vacuum/dry N_2 atmosphere delays degradation; P3HT better than spiro-OMeTAD for stable devices; O_2 causes degradation
Degradation of co-evaporated perovskite thin film in air[6]	Moisture and air exposure	XRD, XPS, AFM	$CH_3NH_3PbI_3$/Au coated Si wafer	Decomposition into amorphous C and crystalline PbI_2; $CH_3NH_3PbI_3 + H_2O \rightarrow (-CH_2-) + NH_3(g) + HI(g) + PbI_2$; Degradation leads to film roughening and void creation
Degradation mechanism for planar heterojunction	Air exposure	AFM, PSC, OD	Ag/spiro-OMeTAD /$CH_3NH_3PbI_3$/ TiO_2/ITO	Band gap, morphology change; surface roughness higher in $CH_3NH_3PbI_3$ (v/s $FAPbI_3$) leading to easy attack of water

perovskite solar cells[7]				
Humidity-Induced Grain Boundaries in $MAPbI_3$ Perovskite Films[8]	Humidity	SFM, time resolved in situ XRD	$MAPbI_3$/PEDOT:PSS/ ITO	$MAPbI_3 \cdot H_2O$ under 80 % humidity, reversible under dry N_2 flushing; grain boundaries persisted; partially irreversible degradation to PbI_2 (prolonged humidity exposure)
Structural Phase- and Degradation-Dependent Thermal Conductivity of $CH_3NH_3PbI_3$ Perovskite Thin Films[9]	Moisture	Time-domain thermo-reflectance (TDTR)	$MAPbI_3/Al_2O_3$/glass	Moisture increases the thermal conductivity of $CH_3NH_3PbI_3$film due to formation of PbI_2
Degradation mechanism of $CH_3NH_3PbI_3$ perovskite materials upon exposure to humid air[10]	Humidity	Real time SE, DFT	$CH_3NH_3PbI_3$/ZnO/ Si	Hysteresis ∝ thickness; revival of device performance in dark; Performance instability and hysteresis are not related; performance instability leads to temporary change due to light exposure (proposed)
Reversible Healing Effect of Water Molecules on Fully Crystallized Metal−Halide Perovskite Film[11]	Moisture	Time resolved PL, IS, OD, IV	Au/spiro/$MAPbI_3$/TiO_2/FTO; sprayed without HTM and Au	H_2O improves the quality of film and device performance; H-bonding changes the deep trap states to shallow; healing effect is reversible, though
Stability Comparison of Perovskite Solar Cells Based on Zinc Oxide and Titania on Polymer Substrates[12]	Effect of temperature on substrates- TiO_2 and ZnO	IV, XRD	IZO/ZnO (or TiO_2)/$CH_3NH_3PbI_3$/spiro-MeOTAD/Au	$CH_3NH_3PbI_3$ more stable on TiO_2 than on ZnO
Interface degradation of perovskite solar cells and its modification using an annealing-free TiO_2 NPs layer[13]	Exposure to air	IV	ITO/PEDOT:PSS/$CH_3NH_3PbI_3$/PCBM/Al	Degradation of device and its performance due to Al bubbles formation; TiO_2 prevents bubbles
Degradation of organometallic perovskite solar cells induced by trap states[14]	Ambient atmosphere	PCE, SEM, XRD, OD	FTO/compact TiO_2/$CH_3NH_3PbI_3$ (300 nm)/ HTM/Au	Trap states cause degradation: trap states not caused by HTM, morphology change, conversion to PbI_2 or formation of hydrate
Light and oxygen induced degradation limits the operational stability of methylammonium lead triiodide perovskite solar cells[15]	Light and O_2	PCE, PL	ITO/compact-TiO_2 /meso-TiO_2 /$CH_3NH_3PbI_3$/spiro/Au	Light and O_2 induced degradation (O_2^- responsible) faster than moisture induced; devices degrade in dark under forward bias under O_2 atmosphere
Investigation of the Hydrolysis of	Water	In situ synchrotron	$CH_3NH_3PbI_3$/FTO	Perovskite monohydrate- intermediate of degradation; PbI_2 and CH_3NH_3I are the final

Perovskite Organometallic Halide $CH_3NH_3PbI_3$ in Humidity Environment[16]		radiation XRD, optical microscopy, gravimetry		products of degradation (no conversion to HI or I_2)
Degradation of Methyl ammonium Lead Iodide Perovskite Structures through Light and Electron Beam Driven Ion Migration[17]	Electron beam and laser beam	PL, AFM	$CH_3NH_3PbI_3$/ITO	Electron beam causes ion migration and film thinning; Laser beam causes structural decomposition, spatially scattered particles
Degradation Mechanisms of Solution-Processed Planar PSC: TSC Measurement for Analysis of Carrier Traps[18]	N_2 and ambient atmosphere, light	Thermally stimulated current, PCE, OD	ITO/ PEDOT:PSS/$CH_3NH_3PbI_3$/(α-NPD)/ MoO_3/Al	Perovskite degrades worse in ambient atmosphere than N_2; formation of hole traps in degraded film; source of traps-fragments of photo-degradation in presence of H_2O
Evolution of Chemical Composition, Morphology, and Photovoltaic Efficiency of $CH_3NH_3PbI_3$ Perovskite under Ambient Conditions[19]	Ambient atmosphere	XPS, XRD, SEM, PCE	$CH_3NH_3PbI_3$/FTO; Au/spiro-OMeTAD /$CH_3NH_3PbI_3$/TiO2/FTO	Decomposition to amorphous PbO, $PbCO_3$, $Pb(OH)_2$, crystalline PbI_2 and PbI_{2+x}^{x-} (a proposed degradation mechanism given), I^- and CH_3NH_3I escape; Hysteresis- due to alteration of microstructure
Achieving long-term stable perovskite solar cells via ion neutralization[20]	N_2 atmosphere in glove box and ambient atmosphere	PCE, XPS	ITO/PEDOT:PSS/ VO_x/$MAPbI_{3-x}Br_x$/ $PC_{60}BM$/(Ag or Al).	I^- diffuses and corrodes the counter electrode; amine mediated titanium suboxide b/w PCBM and metal electrode imparts stability to device
Self limiting atomic layer deposition of Al_2O_3 on perovskite surfaces: a reality?[21]	Trimethyl Aluminium (TMA)	In situ FTIR, DFT, XRD, quartz crystal micro-balance	$CH_3NH_3PbI_{3-x}Cl_x$ /Al_2O_3	TMA weakens the interaction b/w PbI_3^- and $CH_3NH_3^+$; ALD growth of Al_2O_3 using TMA and H_2O on perovskite doesn't seem probable
Interfacial Degradation of Planar Lead Halide Perovskite Solar Cells[22]	Light	CV, impedance spectroscopy, 1st principles calculations	ITO/PEDOT:PSS/$CH_3NH_3PbI_3$/PCBM/Al	Cr_2O_3/Cr modification protects cathode; cathode electrical properties change by generation of a dipole which modify interfacial energy barrier leading to impeded electron extraction
Synergistic improvements in stability and performance of lead iodide perovskite solar cells incorporating salt additives[23]	Oxygen and water in glove box; light shocking	PCE, PL	ITO/ PEDOT:PSS/$CH_3NH_3PbI_3$/$PC_{61}BM$/C_{60}/BCP/ Al	KCl and NaCl additives improve crystallinity and coverage of perovskite films, and device performance and stability
Improved air stability of	Water, O_2	Time resolved PL	ITO/ NiO_x/$CH_3NH_3PbI_3$/Zn	NiO_x and ZnO transport layers impart stability to the device

perovskite solar cells via solution-processed metal oxide transport layers[24]			O/ Al	
Photo-induced degradation of lead halide perovskite solar cells caused by the hole transport layer/metal electrode interface[25]	Light	PCE, KPFM, XPS	FTO/compact TiO_2 /$CH_3NH_3PbI_3$/HTM/Au	Photoinduced perovskite degradation is different from light induced device degradation; degradation happens at HTM/Au interface
Low-temperature-processed ZnO–SnO_2 nanocomposite for efficient planar perovskite solar cells[26]	Temperature	PCE, IR	ITO/ZnO-SnO_2/$MAPbI_3$/spiro-OMeTAD/Au	ZnO–SnO_2 nanocomposite thin films exhibit better thermal stability of $CH_3NH_3PbI_3$ and resultant PSC device stability, as compared to ZnO

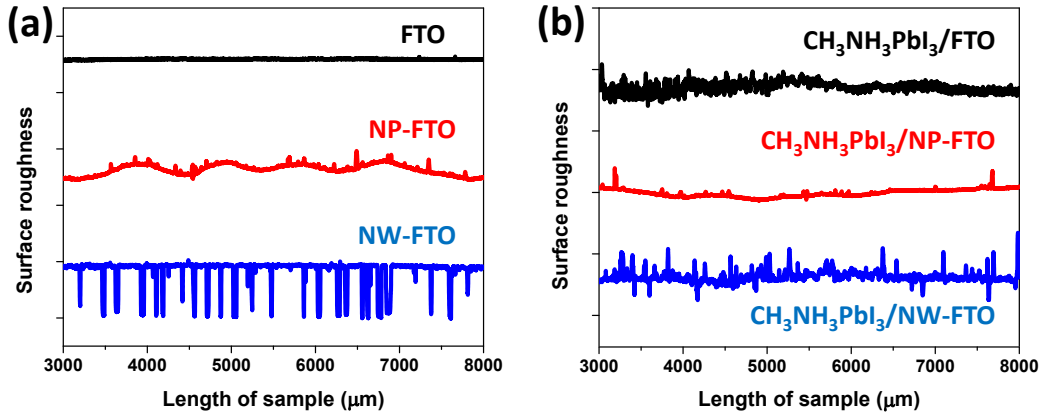

(c)

Substrate	Avg. roughness (nm) before HOIP deposition	Avg. roughness (nm) after HOIP deposition
FTO	32.8	824.3
NP-FTO	470.8	611.1
NW-FTO	1300.8	989.2

Figure S1. Surface profiler line scans of (a) substrates- FTO, NP-FTO, and NW-FTO (the difference between two consecutive divisions on the y-axis = 5 μm), (b) HOIP coated on these substrates (the difference between two consecutive divisions on the y-axis divisions = 10 μm), (c) table showing the average roughness values of these films

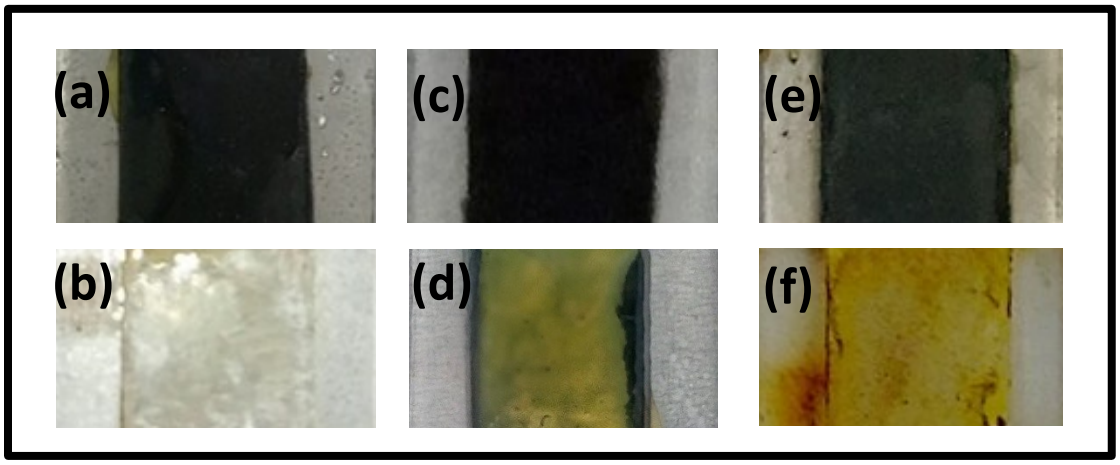

Figure S2. Images of films HOIP coated on (a) and (b) FTO, (c) and (d) NP-FTO, and (e) and (f) NW-FTO. Top row: fresh films; bottom row: degraded films

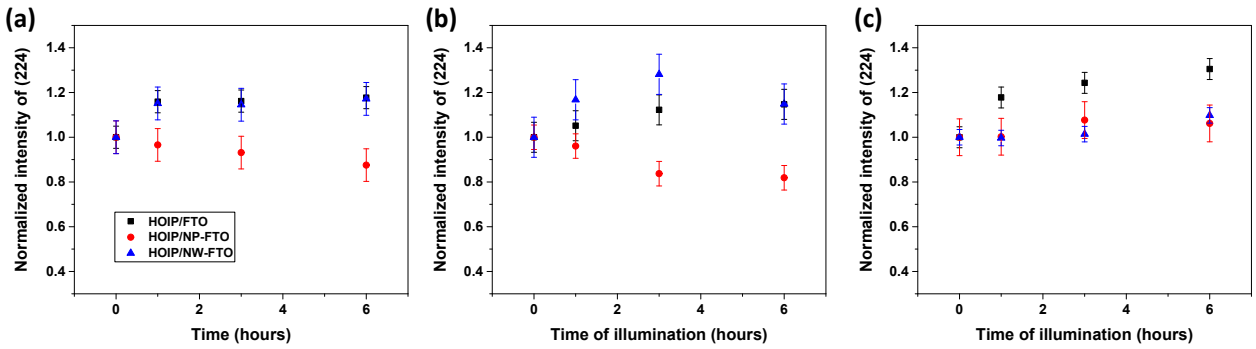

Figure S3. Degradation profiles of HOIP coated on FTO, NP-FTO, and NW-FTO in the initial hours under (a) dark conditions, (b) UV light, and (c) visible light irradiation

Table S2. Full width half maxima (FWHM) values of peaks coming from lattice planes (110) and (310) for HOIP films deposited on FTO, NP-FTO, and NW-FTO when irradiated with 100 W Tungsten lamp (visible light)

HOIP on	Time (h)	FWHM of (110)	FWHM of (310)
FTO	0	0.13 ± 0.0037	0.20 ± 0.0038
	44	0.12 ± 0.0031	0.18 ± 0.0027
NP-FTO	0	0.09 ± 0.0023	0.38 ± 0.0114
	44	0.09 ± 0.0022	0.23 ± 0.0179
NW-FTO	0	0.12 ± 0.0027	0.19 ± 0.0024
	44	0.11 ± 0.0026	0.18 ± 0.0020

Table S3. The ratio of I to Pb in the fresh, degraded and I_2 treated HOIP samples deposited on FTO, NP-FTO, and NW-FTO measured by EDX

HOIP on	Fresh	Degraded	I_2 treated
FTO	2.64	2.62	2.71
NP-FTO	2.73	1.99	1.98
NW-FTO	2.60	2.45	2.64

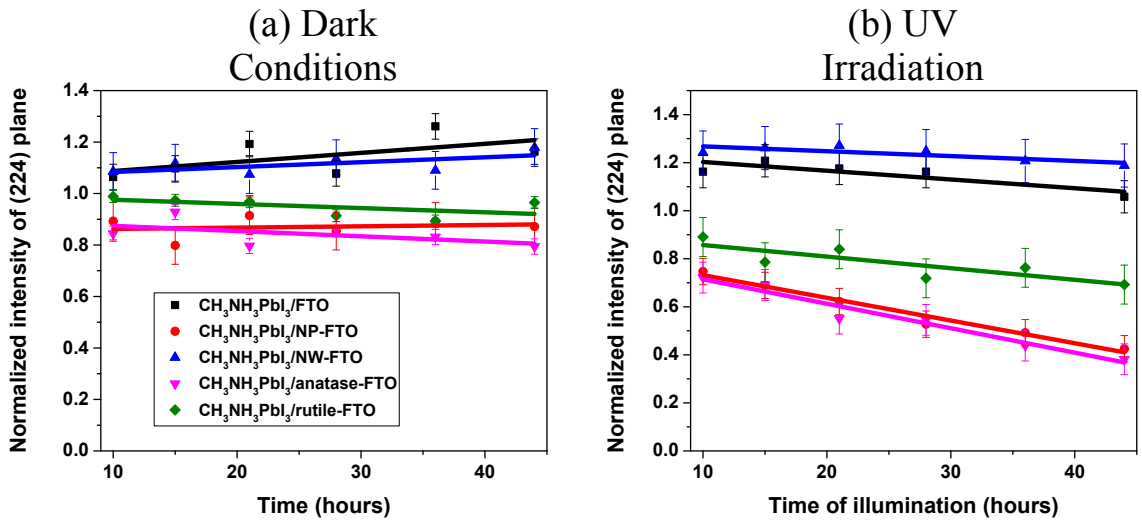

Figure S4. Degradation profiles of HOIP coated on FTO, NP-FTO, and NW-FTO and also HOIP coated on Anatase-FTO and Rutile-FTO, under (a) dark conditions and (b) UV light irradiation.

References

1 E. Smecca, Y. Numata, I. Deretzis, G. Pellegrino, S. Boninelli, T. Miyasaka, A. La Magna and A. Alberti, *Phys. Chem. Chem. Phys.*, 2016, **18**, 13413-13422.

2 J. Idígoras, A. Todinova, J. Sánchez-Valencia, A. Barranco, A. Borrás and J. Anta, *Phys. Chem. Chem. Phys.*, 2016, **18**, 13583-13590.

3 W. Nie, J. Blancon, A. Neukirch, K. Appavoo, H. Tsai, M. Chhowalla, M. Alam, M. Sfeir, C. Katan, J. Even, S. Tretiak, J. Crochet, G. Gupta and A. Mohite, Nature Communications, 2016, 7, 11574.

4 F. Liu, Q. Dong, M. Wong, A. Djurišić, A. Ng, Z. Ren, Q. Shen, C. Surya, W. Chan, J. Wang, A. Ng, C. Liao, H. Li, K. Shih, C. Wei, H. Su and J. Dai, *Advanced Energy Materials*, 2016, **6**, 1502206.

5 Y. Dkhissi, H. Weerasinghe, S. Meyer, I. Benesperi, U. Bach, L. Spiccia, R. Caruso and Y. Cheng, *Nano Energy*, 2016, **22**, 211-222.

6 C. Wang, Y. Li, X. Xu, C. Wang, F. Xie and Y. Gao, *Chemical Physics Letters*, 2016, **649**, 151-155.

7 K. Yamamoto, Y. Furumoto, M. Shahiduzzaman, T. Kuwabara, K. Takahashi and T. Taima, *Jpn. J. Appl. Phys.*, 2016, **55**, 04ES07.

8 D. Li, S. Bretschneider, V. Bergmann, I. Hermes, J. Mars, A. Klasen, H. Lu, W. Tremel, M. Mezger, H. Butt, S. Weber and R. Berger, *J. Phys. Chem. C*, 2016, **120**, 6363-6368.

9 Z. Guo, S. Yoon, J. Manser, P. Kamat and T. Luo, *J. Phys. Chem. C*, 2016, **120**, 6394-6401.

10 M. Shirayama, M. Kato, T. Miyadera, T. Sugita, T. Fujiseki, S. Hara, H. Kadowaki, D. Murata, M. Chikamatsu and H. Fujiwara, *J. Appl. Phys.*, 2016, **119**, 115501.

11 W. Zhou, Y. Zhao, C. Shi, H. Huang, J. Wei, R. Fu, K. Liu, D. Yu and Q. Zhao, *J. Phys. Chem. C*, 2016, **120**, 4759-4765.

12 Y. Dkhissi, S. Meyer, D. Chen, H. Weerasinghe, L. Spiccia, Y. Cheng and R. Caruso, *ChemSusChem*, 2016, **9**, 687-695.

13 J. Xiong, B. Yang, C. Cao, R. Wu, Y. Huang, J. Sun, J. Zhang, C. Liu, S. Tao, Y. Gao and J. Yang, *Organic Electronics*, 2016, **30**, 30-35.

14 D. Song, J. Ji, Y. Li, G. Li, M. Li, T. Wang, D. Wei, P. Cui, Y. He and J. Mbengue, *Appl. Phys. Lett.*, 2016, **108**, 093901.

15 D. Bryant, N. Aristidou, S. Pont, I. Sanchez-Molina, T. Chotchuangchutchaval, S. Wheeler, J. Durrant and S. Haque, *Energy Environ. Sci.*, 2016, **9**, 1655-1660.

16 J. Zhao, B. Cai, Z. Luo, Y. Dong, Y. Zhang, H. Xu, B. Hong, Y. Yang, L. Li, W. Zhang and C. Gao, *Sci. Rep.*, 2016, **6**, 21976.

17 H. Yuan, E. Debroye, K. Janssen, H. Naiki, C. Steuwe, G. Lu, M. Moris, E. Orgiu, H. Uji-i, F. De Schryver, P. Samori, J. Hofkens and M. Roeffaers, *J. Phys. Chem. Lett.*, 2016, **7**, 561-566.

18 C. Qin, T. Matsushima, T. Fujihara, W. Potscavage and C. Adachi, *Adv. Mater.*, 2015, **28**, 466-471.

19 W. Huang, J. Manser, P. Kamat and S. Ptasinska, *Chemistry of Materials*, 2016, **28**, 303-311.

20 H. Back, G. Kim, J. Kim, J. Kong, T. Kim, H. Kang, H. Kim, J. Lee, S. Lee and K. Lee, *Energy Environ. Sci.*, 2016, 9, 1258-1263.

21 D. Choudhury, G. Rajaraman and S. Sarkar, *Nanoscale*, 2016, **8**, 7459-7465.

22 A. Guerrero, J. You, C. Aranda, Y. Kang, G. Garcia-Belmonte, H. Zhou, J. Bisquert and Y. Yang, *ACS Nano*, 2016, **10**, 218-224.

23 K. Boopathi, R. Mohan, T. Huang, W. Budiawan, M. Lin, C. Lee, K. Ho and C. Chu, *J. Mater. Chem. A*, 2016, **4**, 1591-1597.

24 J. You, L. Meng, T. Song, T. Guo, Y. Yang, W. Chang, Z. Hong, H. Chen, H. Zhou, Q. Chen, Y. Liu, N. De Marco and Y. Yang, *Nature Nanotech*, 2015, **11**, 75-81.

25 D. Wei, T. Wang, J. Ji, M. Li, P. Cui, Y. Li, G. Li, J. Mbengue and D. Song, *J. Mater. Chem. A*, 2016, **4**, 1991-1998.

26 J. Song, E. Zheng, X. Wang, W. Tian and T. Miyasaka, *Solar Energy Materials and Solar Cells*, 2016, **144**, 623-630.